Fractional Charge Revealed in Computer Simulations of Resonant Tunneling in the Fractional Quantum Hall Regime

E. V. Tsiper*

School of Computational Sciences, George Mason University, Fairfax, Virginia 22030, USA
Center for Computational Materials Science, Naval Research Laboratory, Washington, D.C. 20375, USA

(Received 15 August 2005; published 15 August 2006)

The concept of fractional charge is central to the theory of the fractional quantum Hall effect. Here I use exact diagonalization as well as configuration space renormalization to study finite clusters which are large enough to contain two independent edges. I analyze the conditions of resonant tunneling between the two edges. The ''computer experiment'' reveals a periodic sequence of resonant tunneling events consistent with the experimentally observed fractional quantization of electric charge in units of $e/3$ and $e/5$.

DOI: 10.1103/PhysRevLett.97.076802 PACS numbers: 73.43.Cd

Perhaps the most intriguing feature of the fractional quantum Hall effect (FQHE) [1] is the existence of quasiparticles whose electric charge is a simple fraction of the elementary charge e [2]. Quasiparticles of charge $e^* = e/3$ and $e/5$ have been first observed experimentally in the $\nu = \frac{1}{3}$ and $\nu = \frac{2}{5}$ fractional states, respectively, using resonant tunneling via a quantum antidot (a potential hill) [3–5].

Since the bulk fractional state is an insulator, the most interesting transport properties of the system are associated with the edges, particularly with tunneling into or between the edges [3–8]. Because of cluster size limitations, computational studies of edge physics have focused on the properties of a single edge, such as nonuniversality of the tunneling exponent [9,10] or reconstruction of the charge density [11–14]. The properties of the Laughlin wave function describing a dual-edge system have been studied in cylindrical [15] and disk geometries [16]. Study of edge to edge tunneling through a bulk fractional state requires clusters large enough to contain two independent edges.

Exact diagonalization (ED) of finite clusters has been very fruitful in helping to understand the physics of FQHE [2,9–16]. Ordinary electronic structure methods fail for this system because the kinetic energy is quantized by the magnetic field. ED, or ''full CI'' in quantum chemical terminology, imposes severe restrictions on the cluster size, since the dimensionality of the Hilbert space grows exponentially with the number of particles N:

$$\binom{L}{N} \approx \frac{1}{\sqrt{2\pi L f(1-f)}}\left[\frac{1}{f^f(1-f)^{(1-f)}}\right]^L. \qquad (1)$$

Here $L = N/f$, $f < 1$, is the *filling factor*. The quantity in brackets reaches a maximum value of 2 at $f = \frac{1}{2}$.

In the past, we have perfected the Lanczos technique [17,18], both Hermitian [19,20] and not [21–23], to work with matrices up to $\sim 10^9 \times 10^9$. Equation (1) translates this into about $N = 12$ particles at $f = \frac{1}{3}$ or $N = 16$ at $f = \frac{1}{2}$. Whereas exact solutions for up to $N = 22$ are sometimes possible [20], $N \gtrsim 12$ normally require approximate methods. Here I use ED and also an approximate method to model the resonant tunneling experiments [3–5].

In Refs. [3–5], a periodic sequence of *resonant tunneling events* was observed as either the magnetic field H or the backgate voltage V_{BG} was varied. The tunneling events are thought of in terms of a quasiparticle tunneling through the bulk of the fractional state between the outer edge of the sample and the inner edge formed around the antidot. The periodicities ΔH and ΔV_{BG} were related [3] to the quasiparticle charge e^*.

In order to mimic the experimental setup, I consider a planar FQHE sample with two unconnected edges (inset in Fig. 1). N electrons in the lowest Landau level are confined by the potential of a uniformly charged disk with a hole in the center, positioned in the plane of the two-dimensional (2D) electron gas. The positive charge density σ and the inner radius R_1 of the disk are free parameters. The outer radius R_2 is always chosen such that the whole system is neutral. The electronic density $\rho(r)$ confines itself between R_1 and R_2, falling off sharply beyond this range. Setting σ to a fraction $\nu = \frac{1}{3}, \frac{2}{5}$, etc., of the density σ_1 of the completely filled Landau level controls the fractional state, with $\rho(r)$ approaching $\nu\sigma_1$ (for $N \to \infty$) far from both edges. Near the edges, $\rho(r)$ is known to exhibit oscillatory behavior thought to decay slowly into the bulk [13]. Such behavior prevents formation of a well-defined density plateau between the edges in the finite clusters studied here numerically.

An increase in R_1 strengthens the antidot and expels a charge from inside of the antidot towards the outer edge. The charge expelled does not accumulate in the bulk because of neutrality considerations and because of incompressibility of the bulk fractional state. I prefer to use the ''missing charge'' $Q = \sigma\pi R_1^2/e$ as a variable, instead of R_1. When Q is continuously increased, the ground state of the system reconstructs via a steplike process. The reconstruction events correspond to ground-state degeneracies, when it costs no energy to transfer charge from the inner to the outer edge. This is precisely the condition for resonant tunneling through the antidot.

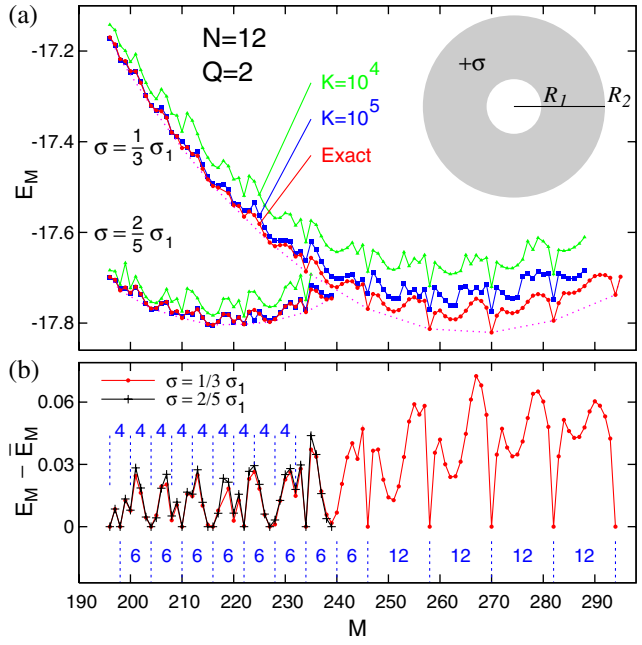

FIG. 1 (color online). Exact ground-state energy of $N = 12$ electrons in 2D confined by Coulomb attraction to a uniformly charged annulus (inset) of charge density $\sigma = \frac{1}{3}$ and $\frac{2}{5}$ of the filled Landau level. The units are e^2/ℓ_H. The upper panel also shows CSR results for $K = 10^4$ and 10^5. Full Hilbert space dimensionality is 10^8–10^9 and varies with M [34]. The 2/5 data are shifted upward by 1.5. The lower panel exposes the FQHE-related structure in E_M by subtracting the greatest convex minorant $\bar{E}_M$ [the dotted purple line].

In the disk geometry, the single-particle states ψ_m in the lowest Landau level are characterized by the angular momentum $m = 0, 1, \ldots$, and the total angular momentum $M = \sum m$ is conserved. The Coulomb matrix elements are known [24,25]. The matrix elements of the confining potential are $V_m = V_m(R_2) - V_m(R_1)$, where

$$V_m(R) = \iint_{\rho<R} d^2\rho d^2 r \frac{e\sigma}{|\mathbf{r}-\boldsymbol{\rho}|}|\psi_m(r)|^2 = (2\pi)^{3/2} e\sigma\ell_H Z e^{-Z} \sum_{i=0}^{m} [q^-_{im} I_0(Z) + q^+_{im} I_1(Z)] Z^i. \tag{2}$$

Here $\ell_H = \sqrt{\hbar c/eH}$ is the magnetic length, $Z = R^2/4\ell_H^2$, $q^{\pm}_{00} = 1$, $q^{\pm}_{0m} = (2m \pm 1) q_{0,m-1}$, and $q^{\pm}_{im} = (2m - 2i \pm 1) q^{\pm}_{i,m-1} + 2q^{\mp}_{i-1,m-1} - 2q^{\mp}_{i-1,m-1}$.

For a given set of N, Q, and σ, I find the lowest energy $E_M(Q)$ at each M. The ground-state energy is then $E(Q) = \min E_M(Q)$. The ground-state reconstruction events occur via level crossings of branches with different M and lead to a stepwise function $M(Q)$. The number p of the steps that occur per $\Delta Q = 1$ may be related to the charge e/p that is moved from the inner to the outer edge per one reconstruction event.

Figure 1 shows $E_M(Q)$ for $N = 12$, $Q = 2$. The sequence of sharp cusps on the right curve are the $\frac{1}{3}$ fractional states. The state at $M = 270$ is the true ground state at $Q = 2$ and $\sigma = \frac{1}{3}\sigma_1$, whereas the states with $M = 270 \pm 12$, $M = 270 \pm 24$, etc., are candidates for the ground state at different Q. The quasiperiodicity with $\Delta M = 12$ is due to the approximate invariance of the antidot Hamiltonian with respect to the Laughlin's quasihole creation operator [2] $\mathcal{A}_0$, also known to be the generator of infinitesimal magnetic translations [26]. Applied to an arbitrary many-electron wave function Ψ, it translates it in the angular momentum space, $m \to m + 1$. The total angular momentum then transforms as $M \to M + N$:

$$\Psi_{M+N} \approx \mathcal{A}_0 \Psi_M. \tag{3}$$

At $Q = 0$, the ground state occurs, approximately, at the Laughlin's angular momentum [27]

$$M^*(Q = 0) = \frac{N(N-1)}{2\nu}. \tag{4}$$

I generalize this for a disk with the missing charge Q as

$$M^* = \frac{(N+Q)(N+Q-1)}{2\nu} - \frac{Q(Q-1)}{2\nu}. \tag{5}$$

For $N = 12$, $Q = 2$, I get $M^*_{1/3} = 270$ and $M^*_{2/5} = 225$ (cf. Fig. 1).

The single-particle orbitals $\psi_m(r)$ are localized near $r = \ell_H\sqrt{2m}$, where ℓ_H is the magnetic length. Therefore, in a macroscopic system whose density approaches a constant $\nu\sigma_1$ in the bulk, the operator $\mathcal{A}_0$ pushes the density out of the center, creating an effective positive charge $e^* = \nu e$. This is an exact formal property of $\mathcal{A}_0$ but relates to the physical system via the approximate invariance (3). Indeed, Eq. (5) can be obtained from (4) by applying $\mathcal{A}_0^{(Q/\nu)}$:

$$M^* = M^*(Q = 0) + NQ/\nu. \tag{6}$$

Figure 1, therefore, suggests that the ground state of the $\frac{1}{3}$ system changes in steps of $\Delta M = N$, transferring charge $e^* = e/3$ from the inner to the outer edge at every step. According to (6), the steps should occur at $\Delta Q \approx \nu = \frac{1}{3}$.

Remarkably, the range of M that corresponds to the $\frac{2}{5}$ fractional state exhibits double periodicity, $\Delta M = 6 = N/2$. This should cause branch crossings twice as often, $\Delta Q \approx \nu/2 = 1/5$. Consequently, the charge transferred per one reconstruction event is $e^* = \nu e/2 = e/5$, in agreement with the experiment [4]. The double periodicity in $E_M(Q)$ at $\sigma = \frac{2}{5}\sigma_1$ shows up also for $N = 11$, 10, 9, and 8, though it is less pronounced for smaller N.

Figure 1(b) exposes the tiny structure in $E_M(Q)$ by subtracting its greatest convex minorant $\bar{E}_M$ [dotted purple line in Fig. 1(a)]. I notice that this structure, which is the manifestation of the FQHE, is insensitive to the confining potential and is practically the same for $\sigma = \frac{1}{3}\sigma_1$ and $\frac{2}{5}\sigma_1$, suggesting rigidity of the wave function with respect to the

confining potential [$\delta\Psi_M/\delta V(r)$ being small by some measure], whereas the principal effect of $V(r)$ is to select which M is the ground state. Figure 1(b) also suggests that traces of $\Delta M = 4$ periodicity may be present in the area near $M^*_{3/7} = 210$. By the same logic, $\Delta M = N/3$ at $\frac{3}{7}$ filling corresponds to $e^* = e/7$, although larger clusters are needed to separate the $\frac{2}{5}$ and $\frac{3}{7}$ states. Indeed, from Eq. (4), the condition $M^*_{2/5} - M^*_{3/7} \geq N$ leads, at $Q = 0$, to $N \geq 13$.

I further use the configuration space renormalization (CSR) approach to study larger clusters up to $N = 15$ and to compute $E_M(Q)$ for several values of Q and obtain the branch crossings directly. The CSR reduces the dimensionality of the many-body Hilbert space by selecting its most relevant subspace. It is similar in spirit to the basis set reduction ("BSR") technique by Wenzel and Wilson [28] and a number of related algorithms [29–32]. The CSR iteratively improves a basis set of K many-body configurations using their weight in the solution as the criterion of relevance.

The CSR algorithm works as follows. I start with an arbitrary set of K many-body configurations and diagonalize the Hamiltonian in the subspace they span. The result is a state vector expanded in many-body configurations. I then retain $K' < K$ configurations by discarding the ones which have little weight. I reexpand the set with the new configurations that have large matrix elements with those retained. When repeated, the procedure converges after 10–15 iterations (Fig. 2) and yields some optimal set of configurations.

The resulting basis truncation is essentially many-body and cannot be achieved by truncating or rotating the single-particle basis. ED performed in the subspace yields a variationally stable ground-state energy that converges to the exact value as K is increased. In practice, I do not keep K constant but increase it from iteration to iteration (Fig. 2, inset), monitor the convergence, and extrapolate as $1/K \to 0$ [33].

Figure 1 compares CSR results for $K = 10^4$ and 10^5 against the exact solution. We see that the essential FQHE structure survives the basis truncations of several orders of magnitude and that a reasonable accuracy is achieved for $K = 10^5$ in the whole range of M. Qualitative results are obtained already with K as small as 10^4.

I used CSR to compute $E_M(Q)$ for Q in steps of 0.25, interpolated between these points with a cubic spline, and found $\min E_M(Q)$ over M at every Q (Fig. 3). I used $K = 200\,000$ for $N \leq 13$, $K = 500\,000$ for $N = 14$, and $K = 1\,000\,000$ for $N = 15$. K was doubled in some calculations where the extrapolation to $1/K \to 0$ seemed ambiguous.

Figure 3 shows steps $M(Q)$ for N from 11 through 15, as the missing charge Q is continuously increased. The left panel shows that three steps typically occur per $\Delta Q = 1$ for all N. The general slope is consistent with Eq. (6), and most of the steps in the left panel have $\Delta M = N$ precisely. The data for the $2/5$ fraction (the middle panel) show steps occurring about twice as often. These observations are in line with our expectations based on the quasiperiodicities seen in Fig. 1. Careful examination of the $\frac{2}{5}$ data shows that the change $M \to M + N$ occurs usually in two steps,

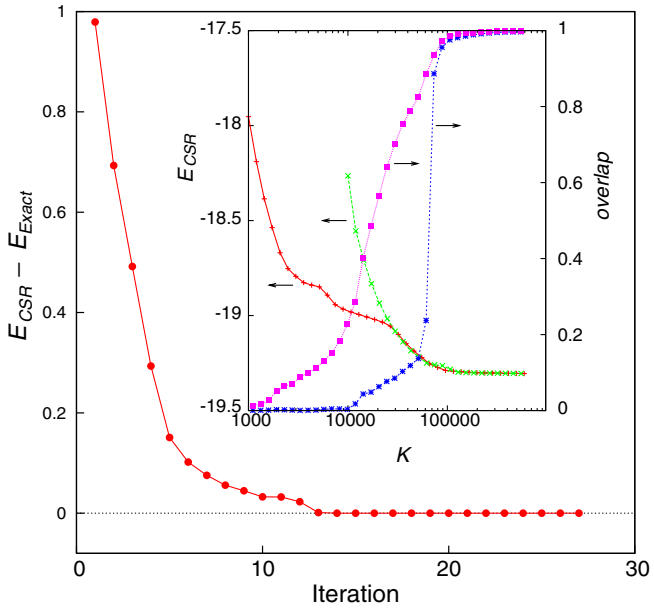

FIG. 2 (color online). Typical CSR energy convergence, $N = 12$, $\sigma = \frac{2}{5}\sigma_1$, $M = 216$, $K = 10^5$. The inset shows convergence with K when K is increased by a factor of 1.2 at every iteration. "+" (red) and "×" (green) data sets indicate insignificance of the starting value of K except for the initial iterations. The stars (blue) give the overlap with the exact eigenvector. The squares (purple) show the magnitude of projection of the exact eigenvector onto the CSR subspace (that is, maximum overlap with any vector in the subspace) and as such characterize the quality of the subspace [36].

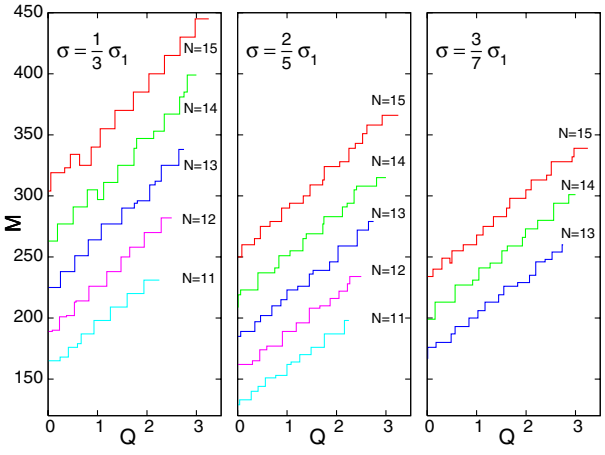

FIG. 3 (color online). Angular momentum $M(Q)$ of the ground-state changes in steps as the missing charge Q is tuned continuously. The steps occur at the ground-state degeneracies, when it costs no energy to move a quasiparticle from the inner to the outer edge, and can be associated with the resonant tunneling between the edges through the bulk of the FQH state.

although these steps are not always equal to $N/2$. The data for $\frac{3}{7}$ have been computed only for $N \geq 13$ as discussed above. They show behavior similar to the $\frac{2}{5}$ data. An expectation of 7 steps per $\Delta Q = 1$ (or $\Delta M = N/3$ as we would expect for $e^* = e/7$) cannot be confirmed. This could mean that the $N = 15$ cluster size is not large enough to distinguish the $\frac{3}{7}$ fraction. It could also indicate a genuine property of the $\frac{3}{7}$ fraction that needs to be understood.

In conclusion, I have conducted a ''computer experiment'' designed to model the key elements of the real experiment on resonant tunneling through a quantum antidot [3]. The data on small clusters obtained using ED and CSR reveal a sequence of the ground-state reconstruction events consistent with the periodicity of the resonant tunneling peaks observed experimentally.

The CSR approach employed here offers a number of advantages in modeling many-body clusters. In particular, truncation of the single-particle basis, whenever possible (such as restricting the range of m [34]) occurs automatically within CSR, which discards irrelevant many-particle configurations and thus effectively removes any single-particle state that contributes to none of the relevant configurations. This feature itself can be a major simplification, because the relevance of a single-particle orbital cannot always be judged in advance.

The term ''renormalization'' I use reflects the spirit of the renormalization theory, yet I have not observed any defined fixed point: The set of K relevant configurations keeps changing slightly upon convergence, with some marginally relevant configurations being replaced with other similarly relevant ones.

In general, performance of CSR may benefit if it is augmented with rotations of the single-particle basis [35], though the choice of the basis is fixed by symmetry in the case of the lowest Landau level in disk geometry.

I thank V. J. Goldman for numerous enlightening conversations. I also acknowledge stimulating discussions with A. L. Aleiner.

*Electronic address: etsiper@gmu.edu

[1] D. C. Tsui, H. L. Stormer, and A. C. Gossard, Phys. Rev. Lett. **48**, 1559 (1982).
[2] R. B. Laughlin, Phys. Rev. Lett. **50**, 1395 (1983).
[3] V. J. Goldman and B. Su, Science **267**, 1010 (1995).
[4] V. J. Goldman, Surf. Sci. **361**, 1 (1996).
[5] V. J. Goldman, Physica (Amsterdam) **1E**, 15 (1998).
[6] A. M. Chang, Rev. Mod. Phys. **75**, 1449 (2003).
[7] A. Boyarsky, V. V. Cheianov, and O. Ruchayskiy, Phys. Rev. B **70**, 235309 (2004).
[8] S. Khlebnikov, Phys. Rev. B **73**, 045331 (2006).
[9] X. Wan, F. Evers, and E. H. Rezayi, Phys. Rev. Lett. **94**, 166804 (2005).
[10] V. J. Goldman and E. V. Tsiper, Phys. Rev. Lett. **86**, 5841 (2001).
[11] S. Mitra and A. H. MacDonald, Phys. Rev. B **48**, 2005 (1993).
[12] X. Wan, K. Yang, and E. H. Rezayi, Phys. Rev. Lett. **88**, 056802 (2002).
[13] E. V. Tsiper and V. J. Goldman, Phys. Rev. B **64**, 165311 (2001).
[14] G. S. Jeon and J. K. Jain, Phys. Rev. B **71**, 045337 (2005).
[15] E. H. Rezayi and F. D. M. Haldane Phys. Rev. B **50**, 17 199 (1994).
[16] S.-R. E. Yang, S. Mitra, A. H. MacDonald, and M. P. A. Fischer, J. Korean Phys. Soc. **29**, S10 (1996).
[17] C. Lanczos, J. Res. Natl. Bur. Stand. **45**, 255 (1950).
[18] B. N. Parlett, *The Symmetric Eigenvalue Problem* (Prentice-Hall, London, 1980).
[19] E. V. Tsiper and A. L. Efros, Phys. Rev. B **57**, 6949 (1998).
[20] E. V. Tsiper and A. L. Efros, J. Phys. Condens. Matter **9**, L561 (1997).
[21] E. V. Tsiper, Pis'ma Zh. Eksp. Teor. Fiz. **70**, 740 (1999) [JETP Lett. **70**, 751 (1999)].
[22] V. Chernyak *et al.*, J. Chem. Phys. **113**, 36 (2000).
[23] E. V. Tsiper, J. Phys. B **34**, L401 (2001).
[24] S. M. Girvin and T. Jach, Phys. Rev. B **28**, 4506 (1983).
[25] E. V. Tsiper, J. Math. Phys. (N.Y.) **43**, 1664 (2002).
[26] Yu. A. Bychkov and E. I. Rashba, Zh. Eksp. Teor. Fiz. **90**, 346 (1986) [Sov. Phys. JETP **63**, 200 (1986)].
[27] C. Yannouleas and U. Landman, Phys. Rev. B **68**, 035326 (2003).
[28] W. Wenzel and K. G. Wilson, Phys. Rev. Lett. **69**, 800 (1992).
[29] P. J. Knowles and N. C. Handy, J. Chem. Phys. **91**, 2396 (1989).
[30] J. Riera and E. Dagotto, Phys. Rev. B **47**, R15 346 (1993).
[31] F. G. Pikus and A. L. Efros, Solid State Commun. **92**, 485 (1994).
[32] N. A. Modine and E. Kaxiras, Phys. Rev. B **53**, 2546 (1996).
[33] Technically, the basis expansion procedure is possible since the Hamiltonian matrix is sparse and has a limited number of matrix elements for each row (configuration). I ''expand'' the configurations one by one in the order of decreasing their weight. For each configuration, a number of new configurations related to it by a matrix element is formed and added to the basis. The process continues until the target K is achieved, and all the remaining unexpanded configurations are discarded. In order to enhance the K'/K ratio, I limit the number of new configurations by considering only the matrix elements with $\Delta m = \pm 1$. Different schemes for choosing ''large'' matrix elements are possible and yield similar results.
[34] The calculations were performed on a Pentium 4 workstation. ED results in Fig. 1 had single-particle angular momenta restricted to empirically found interval $(M - M^* + 1)/N - 1 \leq m \leq (M - M^* - 1)/N + 3N - 2$, beyond which the occupation numbers are small. This restriction reduces the actual matrix size from $\sim 10^9$ to about 1.6×10^7. In CSR calculations, the above restriction on m is lifted; however, I used $m \leq 50$ for technical reasons.
[35] E. Dagotto, G. B. Martins, J. Riera, A. L. Malvezzi, and C. Gazza, Phys. Rev. B **58**, 12 063 (1998).
[36] The CSR calculation in Fig. 2 took 11 min. A single point ED run for the same cluster ($N = 12$, $M = 216$) took 24 h. The CPU time comparison is meaningful only to a degree, because ED calculations are disk intensive.